Mon. Not. R. Astron. Soc. **292,** 646–650 (1997)

Testing the homogeneous synchrotron self-Compton model for gamma-ray production in Mrk 421

W. Bednarek★ and R. J. Protheroe

Department of Physics and Mathematical Physics, The University of Adelaide, Adelaide, Australia 5005

Accepted 1997 July 22. Received 1997 July 15; in original form 1997 April 22

ABSTRACT

Based on the detected variability time-scales of X-ray and TeV gamma-ray emission, and the observed multiwavelength photon spectrum, of Mrk 421 we place constraints on the allowed parameter space (magnetic field and Doppler factor of the emission region) for the homogeneous synchrotron self-Compton model. The spectra calculated for the allowed parameters are marginally consistent with the available spectral information above ~ 1 TeV reported by the Whipple Observatory in the case of a 1-d flare time-scale. However, for the recently reported very short duration flares varying on a time-scale of 15 min, the calculated spectra are significantly steeper, suggesting that the homogeneous synchrotron self-Compton model has problems in describing the relatively flat observed spectra extending above a few TeV. We determine the maximum ratio of TeV gamma-ray luminosity to X-ray luminosity during flaring that is allowed by the homogeneous synchrotron self-Compton model for the case of no significant photon–photon absorption in the source.

Key words: radiation mechanisms: non-thermal – galaxies: active – galaxies: individual: Mrk 421 – galaxies: jets – gamma-rays: theory.

1 INTRODUCTION

Very high-energy (VHE) γ-ray emission has been detected in recent years from two BL Lac objects Mrk 421 (Punch et al. 1992; Petry et al. 1996) and Mrk 501 (Quinn et al. 1996). The emission varies significantly on different time-scales, from weeks and days (Kerrick et al. 1995; Schubnell et al. 1996; Buckley et al. 1996) to fractions of an hour (Gaidos et al. 1996). Multiwavelength observations of Mrk 421 show that the TeV γ-ray flares are simultaneous with the X-ray flares observed by the *ASCA* satellite, and that the power emitted in these two energy ranges is comparable (Macomb et al. 1995; Takahashi et al. 1996; Buckley et al. 1996). However during this same period, the amplitude of variations in the lower energy emission (UV–optical) and the γ-ray emission in the EGRET energy range was much less than that of the VHE γ-ray emission (Lin et al. 1994; Macomb et al. 1995; Buckley et al. 1996). VHE emission from Mrk 421 has been observed up to ~ 4 TeV in the quiescent state (Mohanty et al. 1993), and up to at least ~ 8 TeV in the high state (Krennrich et al. 1997). Emission extending to similar energies has also been observed recently from Mrk 501 (Breslin et al. 1997). Summing the HEGRA array data from several nearby blazars (including Mrk 421) there is some evidence (6.5σ) of γ-ray emission above 50 TeV (Meyer & Westerhoff 1996; Meyer, private communication), and for Mrk 421 alone the significance is 3.8σ.

Gamma-ray emission from active galactic nuclei (AGN) is often interpreted in terms of the homogeneous 'synchrotron self-Compton model' (SSC) in which the low-energy emission (from radio to X-rays) is synchrotron radiation produced by electrons that also up-scatter these low-energy photons into high-energy γ-rays by inverse Compton scattering (ISC) (Macomb et al. 1995; Inoue & Takahara 1996; Bloom & Marscher 1996; Mastichiadis & Kirk 1997). In this model all the radiation comes from this same region in the jet. Such a picture can naturally explain synchronized variability at different photon energies. More complicated (inhomogeneous) SSC models are also proposed which postulate that the radiation at different energies is produced in dif-

★Permanent address: University of Łódź, 90-236 Łódź, ul. Pomorska 149/153, Poland.

ferent regions of the jet (e.g. Ghisellini et al. 1985; Maraschi, Ghisellini & Celotti 1992). It has also been argued that the γ-ray emission from Mrk 421 can be explained by electrons scattering in the Klein–Nishina regime (Zdziarski & Krolik 1993).

Photon–photon pair production on the infrared background radiation was expected to prevent observation above ~ 1 TeV. The observation of γ-rays from Mrk 421 up to 8 TeV without a cut-off in the spectrum, and certainly up to 50 TeV, was unexpected based on calculations for reasonable models of the infrared radiation field (see e.g. Stecker & De Jager 1997 and references therein). Even if cascading is included in the infrared background (Protheroe & Stanev 1993; Entel & Protheroe 1995) observations of γ-rays of these energies seemed unlikely. However, the infrared background is not well known and it may be possible to observe the nearest blazars up to energies somwhat below ~ 100 TeV where absorption on the cosmic microwave background will give a sharp cut-off. In our calculations below, we shall therefore neglect photon–photon pair production on the infrared background.

The purpose of this paper is to confront the homogeneous SSC model with the results of recent observations and, if possible, to derive the parameters of the emission region in the jet from which this radiation originates, i.e. its Doppler factor and magnetic field strength.

2 CONSTRAINTS ON A HOMOGENEOUS SSC MODEL

Let us consider relativistic electrons confined in a 'blob' that moves along the jet with the Doppler factor D and has magnetic field B. In the homogeneous SSC model the radii of the emission regions of low-energy photons (r_1), X-ray photons (r_X) and TeV γ-rays (r_γ) are the same. This region is constrained by the variability time-scale observed, e.g. in TeV γ-rays, $t_{\rm var}$(s),

$$r_1 = r_\gamma = r_X \approx 0.5cDt_{\rm var}. \tag{1}$$

The differential photon density in the blob frame of low-energy synchrotron photons (photon $\mathrm{MeV}^{-1}\,\mathrm{cm}^{-3}$) is then given by

$$n(\epsilon') \approx \frac{4d^2F(\epsilon)}{c^3 t_{\rm var}^2 D^4}, \tag{2}$$

where $d \approx 187$ Mpc is the distance to Mrk 421 (for $H_0 = 50$ km $\mathrm{s}^{-1}\,\mathrm{Mpc}^{-1}$, and $z = 0.031$), $\epsilon = D\epsilon'$ and ϵ' are the photon energies in the observer's and the blob rest frames, and c is the velocity of light.

The differential photon flux in the optical to X-ray region observed from Mrk 421 during the 1994 May 16 flare (photon $\mathrm{cm}^{-2}\,\mathrm{s}^{-1}\,\mathrm{MeV}^{-1}$) can be approximated by a broken power law,

$$F(\epsilon) \approx \begin{cases} b_1\epsilon^{-\beta_1} & 10^{-3}\epsilon_b < \epsilon \le \epsilon_b, \\ b_2\epsilon^{-\beta_2} & \epsilon \ge \epsilon_b, \end{cases} \tag{3}$$

where $\beta_1 = 1.8$, $\beta_2 = 2.3$, $b_1 = 6.9 \times 10^{-4}$ and $b_2 = 2.8 \times 10^{-5}$ are obtained from *ASCA* observations, and $\epsilon_b = 1.65 \times 10^{-3}$ MeV is the energy at which a break in the synchrotron spectrum is observed. Equation (3) is based on the peak 2–10 keV luminosity and spectral index given in fig. 3 of Takahashi et al. (1996) (for $\epsilon > \epsilon_b$), and from fig. 2 of Macomb et al. (1995) we estimate the spectrum for $\epsilon \le \epsilon_b$. Note that for at least 2 decades below $10^{-3}\,\epsilon_b$ the spectrum is uncertain because of the lack of data on the shape of the synchrotron spectrum below $\sim 10^{-9}$ GeV. Because of this, the inverse Compton γ-ray flux in the GeV range will be uncertain and we shall therefore not attempt to predict the GeV flux.

The shape of the synchrotron spectrum defines the shape of the electron spectrum in the blob rest frame, which can be approximated by

$$\frac{dN}{d\gamma'} \approx \begin{cases} a_1\gamma'^{-\alpha_1} & 0.032\gamma'_b < \gamma' \le \gamma'_b, \\ a_2\gamma'^{-\alpha_2} & \gamma' \ge \gamma'_b, \end{cases} \tag{4}$$

where γ' is the Lorentz factor in the blob frame,

$$\gamma'_b = (2\epsilon_b/D\epsilon_B)^{1/2}, \tag{5}$$

$\alpha_1 = 2.6$, $\alpha_2 = 3.6$, $\epsilon_B = m_e c^2 B/B_{\rm cr}$, $B_{\rm cr} = 4.414 \times 10^{13}$ G, m_e is the electron rest mass, $a_1 = a_2/\gamma'_b$, and a_2 can be obtained from fitting the observations. Note that below $10^{-3/2}\gamma'_b = 0.032\gamma'_b$ the spectrum is uncertain.

The spectrum of Mrk 421 shows two clear bumps which, during the outburst stage, extend up to at least ~ 10 keV (Takahashi et al. 1996) and ~ 8 TeV (Krennrich et al. 1997). These multiwavelength observations of Mrk 421 allow us to define the ratio η of the power emitted at a γ-ray energy, E_γ, where the emission is a result of Compton scattering, to the power emitted at an energy, ϵ, where the emission is a result of X-ray synchrotron radiation,

$$\eta = \left(\frac{dN}{dE_\gamma\,dt}E_\gamma^2\right) \Big/ \left(\frac{dN}{d\epsilon\,dt}\epsilon^2\right) = \left(\frac{dN}{dE'_\gamma\,dt'}E'^2_\gamma\right) \Big/ \left(\frac{dN}{d\epsilon'\,dt'}\epsilon'^2\right), \tag{6}$$

where the primed quantities are measured in the blob frame. For the power at γ-ray energies we adopt the value reported for the threshold of the Whipple telescope at $E_\gamma = 0.3$ TeV (Macomb et al. 1995), and for the power at X-ray synchrotron energies we take the value corresponding to the peak emission at $\epsilon = \epsilon_b$ (Takahashi et al. 1996). For these two energies $\eta \approx 1.2$.

The synchrotron spectrum at ϵ' in the above formula (equation 6) can be obtained approximately analytically from the relation

$$\epsilon' \frac{dN}{d\epsilon'dt'}\,d\epsilon' \approx \frac{dN}{d\gamma'}\,d\gamma' b_{\rm syn}(\gamma'), \tag{7}$$

where $dN/d\gamma'$ is the electron spectrum (equation 4). The characteristic energy of synchrotron photons is given by

$$\epsilon' \approx 0.5\epsilon_B\gamma'^2, \tag{8}$$

the energy-loss rate of electrons is $b_{\rm syn}(\gamma') = kU_B\gamma'^2$, where $k = 4c\sigma_T/3$, σ_T is the Thomson cross-section, and $U_B \approx 2.5 \times 10^4 B^2$ (MeV cm^{-3}) is the magnetic field energy density. The synchrotron spectrum emitted by electrons with power-law spectral index α, multiplied by the square of the photon energy, is given by

$$\frac{dN}{d\epsilon'dt'}\epsilon'^2 \approx \frac{2akU_B\epsilon'^2}{\epsilon_B^2}\left(\frac{2\epsilon'}{\epsilon_B}\right)^{-(\alpha+1)/2}. \tag{9}$$

The ICS part of the equation (6) cannot be obtained analytically in the general case because of the complicated form of the Klein–Nishina cross-section, and so we compute this numerically using

$$\frac{dN}{dE'_\gamma dt'} E'^2_\gamma = E'^2_\gamma \int_{\gamma'_{\min}}^{\infty} \frac{dN}{d\gamma'} \int_{\epsilon'_{\min}}^{\infty} \frac{dN(\gamma', E'_\gamma)}{dt' d\epsilon' dE'_\gamma} d\epsilon' d\gamma', \quad (10)$$

where $\gamma'_{\min} \approx E'_\gamma/m_e c^2$, $\epsilon'_{\min} = E'_\gamma/[4\gamma'(\gamma' - E'_\gamma/m_e c^2)]$, $E'_\gamma = E_\gamma/D$, and $dN(\gamma', E'_\gamma)/dt' d\epsilon' dE'_\gamma$ is the ISC spectrum (see equation 2.48 in Blumenthal & Gould 1970) produced by electrons with Lorentz factor γ', which scatter synchrotron photons in the blob having the spectrum given by equations (2) and (3).

Having determined the spectra in equation (6), we can now investigate the parameter space (magnetic field strength in the blob, B, and Doppler factor, D) for the homogeneous SSC model which is consistent with the value of $\eta = 1.2$. In Figs 1(a) and (b) we show the allowed value of B as a function of D (thick full curves) for the case of outbursts as reported by the Whipple Observatory which varied on (a) a ~ 1 d (Buckley et al. 1996; Schubnell et al. 1996) and (b) a ~ 15 min (Gaidos et al. 1996) time-scale.

2.1 Limits from variability time-scales

The variability time-scales observed in TeV γ-rays by the Whipple observatory, and the reports of simultaneous flares observed in X-rays by *ASCA* allow us to place a further constraint on the homogeneous SSC model. A significant decrease in the observed TeV γ-ray and X-ray fluxes may only occur if the electrons have sufficient time to cool during the flare,

$$t'_{\rm cool} \le t_{\rm var} D. \quad (11)$$

This condition is required if the model is truly homogeneous, i.e. the model we consider in the present paper which includes a homogeneous magnetic field and constant jet diretion and bulk Lorentz factor. However, other effects may be responsible for variability of the intensity of X-ray and TeV γ-ray emission such as, for example, a change in angle of motion of the blob, or of its bulk Lorentz factor, or of the magnetic field in the blob. We think that all these possibilities are unlikely as it is very difficult in terms of the SSC model to find a mechanism for a sudden increase (on a time-scale of 15 min) of the Lorentz factor, or of the magnetic field strength in the blob even if magnified by the Doppler factor. A change of the angle motion of the blob with respect to the observer could possibly be caused by an ordered but curved (e.g. helical) magnetic field. However, we must keep in mind that the blob will have a very large inertia because of the high energy density in the blob. In this case, the magnetic field would have to be relatively strong in order to dominate the dynamics of the blob. Relativistic particles would then move preferentially along the ordered magnetic field lines, and the Comptonization of synchrotron photons by this same population of electrons becomes problematic. Therefore, in our opinion (see also Takahashi et al. 1996), the most reasonable explanation of the observed rapid variability of the X-ray and TeV γ-ray emission during flaring in the context of the SSC is as a result of cooling of electrons.

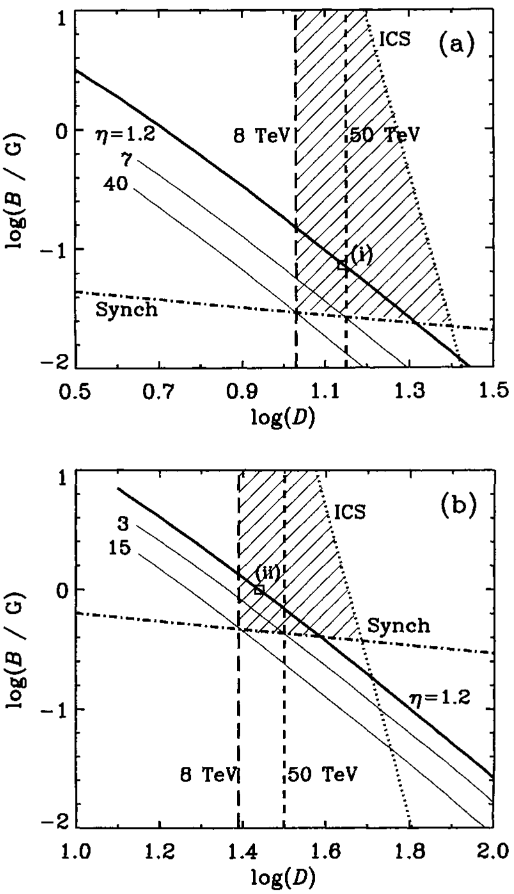

Figure 1. The parameter space (B, D) allowed by the homogeneous SSC model for variability in Mrk 421 on a time-scale $t_{\rm var}$ of (a) 1 d and (b) 15 min. The thick full curves show the condition for $\eta = 1.2$, and the thin full curves (labelled by the value of η) show the condition for other values of η. The other curves give allowed ranges for: efficient cooling of electrons during the flare time-scale by synchrotron radiation (equation 13) – area above dot–dash curve labelled 'Synch'; efficient cooling by ICS (equation 16) – area below dotted curve labelled 'ICS'; escape of 8 TeV γ-rays – area to right of long-dashed curve; escape of 50 TeV γ-rays – area to right of short-dashed curve. The shaded area is the allowed region for the parameters for a spectrum extending to 8 TeV. The representative values of (B, D) that fulfil the condition $\eta = 1.2$ are marked by squares and labelled (i) and (ii).

The cooling time-scale for synchrotron losses of electrons with Lorentz factor γ'_b, which contribute mainly to synchrotron photons at the peak of the spectrum, is given by

$$t'^{\rm syn}_{\rm cool} = \frac{m_e c^2}{k U_B \gamma'_b}. \quad (12)$$

Equations (5), (11) and (12) allow us to place a lower limit on the magnetic field in the blob

$$B > 15.1 t_{\rm var}^{-2/3} \epsilon_b^{-1/3} D^{-1/3}. \quad (13)$$

We next estimate the ICS cooling time and require this to be less than the variability time-scale. For the soft photon spectrum we adopt, some interactions with energetic electrons will be in the Thomson regime, and others will be in the Klein–Nishina regime with relatively small energy loss.

To calculate the cooling time, we neglect interactions in the Klein–Nishina regime, i.e. with photons above $\epsilon'_{\rm T} \approx m_{\rm e}c^2/\gamma'$, and use the simple Thomson energy-loss formula

$$t'^{\rm ICS}_{\rm cool} = \frac{m_{\rm e}c^2}{kU_{\rm rad}(<\epsilon'_{\rm T})\gamma'}, \tag{14}$$

where

$$U_{\rm rad}(<\epsilon'_{\rm T}) \approx \int_0^{\epsilon'_{\rm T}} n(\epsilon')\epsilon'\,{\rm d}\epsilon' \approx 5C\epsilon'^{0.2}_{\rm T}, \tag{15}$$

$C = 4d^2b_1/(c^3t^2_{\rm var}D^{4+\beta_1})$, and we have used the fact that $\epsilon'_{\rm T} < \epsilon'_{\rm b}$ for electrons emitting at TeV energies.

Since the recent report on the Mrk 421 flare observations by the Whipple Observatory gives no evidence of a spectral break at high energies, we assume that the break in the γ-ray spectrum is below but close to the threshold of the Whipple observations, i.e. at ~ 0.3 TeV. This in turn means that electrons with Lorentz factor $\gamma'_{\rm b}$ must cool during the γ-ray flare, and so we shall use $\gamma' = \gamma'_{\rm b}$ in equation (14) to estimate the ICS cooling time-scale. Then, from equations (11) and (14) we can obtain an upper limit on the magnetic field in the blob as a function of Doppler factor, as required by the ICS cooling argument

$$B < 4.4 \times 10^{31}\epsilon_{\beta}t_{\rm var}^{-2.5}D^{-13}. \tag{16}$$

We think that if the X-ray and TeV γ-ray flares are simultaneous, and with comparable energy flux ($\eta \sim 1$) as observed during the flares in Mrk 421 (Buckley et al. 1996), then the energy-loss rates of the highest energy electrons by inverse Compton scattering and synchrotron radiation must be comparable. For blazars in which this is the case, then both the conditions given by equations (12) and (14) must be satisfied simultaneously. On the other hand, if the X-ray flare dominates then equation (14) need not be satisfied, and if the TeV γ-ray flare dominates then equation (12) need not be satisfied.

The constraints on B and D of the blob, derived above (equations 13 and 16), are shown in Figs 1(a) and (b) for the two variability time-scales. In the next section, we derive an additional limit on the Doppler factor of the blob that can be obtained based on the non-observation of absorption of γ-rays by photon–photon pair production with soft photons in the blob radiation.

2.2 Absorption of gamma-rays in the blob radiation

The observation of γ-ray flares with a spectrum extending up to ~ 8 TeV, or even 50 TeV, allows us to place a lower limit on the Doppler factor of the blob under the assumptions of the homogeneous SSC model. Using the observed soft photon spectrum of Mrk 421 (equation 3) we can compute the optical depth $\tau(E'_\gamma, D)$ for γ-ray photons with energy E'_γ for $e^\pm$ pair production inside the blob,

$$\tau(E'_\gamma, D) = \frac{r_\gamma}{8E'^2_\gamma}\int_{\epsilon'_{\rm min}}^{\infty} {\rm d}\epsilon'\,\frac{n(\epsilon')}{\epsilon'^2}\int_{s_{\rm min}}^{s_{\rm max}(\epsilon', E'_\gamma)} {\rm d}s\, s\sigma(s), \tag{17}$$

where $n(\epsilon')$ is the differential photon number density and $\sigma(s)$ is the total cross-section for photon–photon pair production (Jauch & Rohrlich 1955) for a centre of momentum frame energy squared given by

$$s = 2\epsilon' E'_\gamma(1 - \cos\theta') \tag{18}$$

where θ' is the angle between the directions of the energetic photon and soft photon, and

$$s_{\rm min} = (2m_{\rm e}c^2)^2, \tag{19}$$

$$\epsilon_{\rm min} = \frac{(2m_{\rm e}c^2)^2}{4E'_\gamma}, \tag{20}$$

$$s_{\rm max}(\epsilon', E'_\gamma) = 4\epsilon' E'_\gamma. \tag{21}$$

The condition

$$\tau(E'_\gamma, D) < 1, \tag{22}$$

gives us the limit on D. These lower limits are shown by the dashed lines in Figs 1(a) and (b) for variability time-scales $t_{\rm var} = 1$ d and 15 min, and for $E_\gamma = 8$ TeV (long-dashed lines, Krennrich et al. 1997) and 50 TeV (short-dashed lines, Meyer & Westerhoff 1996). The allowed regions of the parameter space (B, D) determined by equations (13), (16) and (22) are shown in Figs 1(a) and (b) by the shaded areas.

3 DISCUSSION AND CONCLUSION

Inspection of the Figs 1(a) and (b) shows that for some values of (B, D), i.e. the region of the thick full line inside the shaded area, the homogeneous SSC model can in principle produce flares with $\eta = 1.2$ as required. We note that the values of (B, D) used in earlier modeling of the Mrk 421 spectrum (Inoue & Takahara 1996; Stecker, De Jager & Salamon 1996; Ghisellini, Maraschi & Dondi 1996; Mastichiadis & Kirk 1997) are generally consistent with the parameter space derived by us. In order to determine if the broad-band spectrum expected in the homogeneous SSC model is consistent with the γ-ray observations during flaring, we compute the synchrotron and ICS spectra for two example parameters (B, D) from the allowed region indicated by points (i) and (ii) in Figs 1(a) and 1(b). The calculated spectra are shown in Fig. 2. Note that in each case, the lowest energy we predict corresponds to $\gamma' = 0.032\gamma'_{\rm b}$ (see equation 4 and comments below), which depends on the magnetic field. For the 2 cases this gives $E'_\gamma \approx 120$ GeV (i) and 47 GeV (ii) for the minimum energies for which we can predict the γ-ray spectrum with any confidence in the homogeneous SSC model.

For energies between 0.8 TeV and 8 TeV corresponding to observations made by the Whipple observatory during recent flaring of Mrk 421 (Krennrich et al. 1997), our predictions of the spectral index in the homogeneous SSC model range from 2.7 for 1-d variability and case (i), to 2.85 for 15-min variability and case (ii). The results obtained during flaring by Krennrich et al. (1997) up to ~ 8 TeV are consistent with the spectrum of Mohanty et al. (1993) taken during a quiescent state where the spectral index was $\sim 2.25 \pm 0.19 \pm 0.3$ between 0.3 and 4 TeV. Given the error bars, this is just consistent with the spectral index of 2.65 predicted for 1-d variability and case (i). However, we note that the calculated spectrum shows a break close to ~ 1 TeV, which should be seen in the Whipple observations.

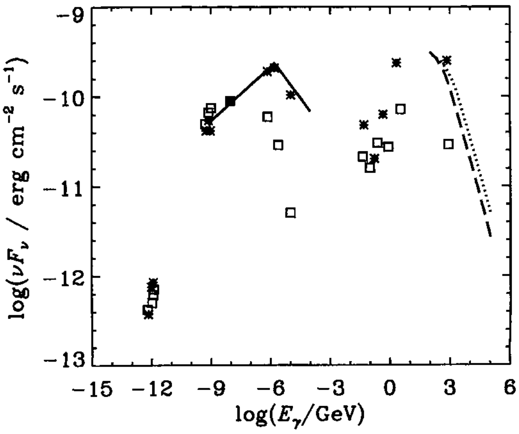

Figure 2. The adopted soft photon spectrum (solid curve at 10^{-9} to 10^{-4} GeV), and the ICS spectra calculated in terms of the homogeneous SSC model for the two representative values of (B, D) of the allowed regions marked by the numbered open squares in Figs 1(a) and (b): (i) dotted curve; (ii) long-dashed curve. Calculated spectra are compared with the observations of Mrk 421 (Macomb et al. 1995) during flaring (asterisk) and in a quiescent state (open squares).

In the case of a flare varying on a 15-min time-scale, it seems that the spectra obtained in terms of the homogeneous SSC model are not consistent with the relatively flat spectrum observed by the Whipple optical Cherenkov telescope. The lower sensitivity HEGRA optical Cherenkov telescope observations report a very steep spectrum above ~ 1 TeV (spectral index $3.6 \pm 1.$) during the 1994 December to 1995 May monitoring (Petry et al. 1996). However these observations refer not to outburst emission, but rather to quiescent emission since the spectrum is integrated over a long period.

In conclusion, detailed spectral measurements in the energy range above 0.3 TeV combined with the observations in the optical–X-ray range should allow one to determine precisely the parameters of the emission region (relativistic blob) and in general answer the question of the applicability of the homogeneous SSC model for γ-ray production in blazars. We note also that the absorption and synchrotron cooling conditions do not allow flares with 1-d variability having $\eta > 40$ (8 TeV) or $\eta > 7$ (50 TeV) – see the thin solid curves in Fig. 1(a). Similarly, for 15-min variability $\eta > 15$ (8 TeV) or $\eta > 3$ (50 TeV) are not allowed (see Fig. 1b). Observation of such huge γ-ray outbursts without accompanying X-ray outbursts would be inconsistent with the homogeneous SSC model.

REFERENCES

Bloom S. D., Marscher A. P., 1996, ApJ, 461, 657
Blumenthal G. R., Gould R. J., 1970, Rev. Mod. Phys., 42, 237
Breslin A. C. et al., 1997, IAU Circ. No. 6592
Buckley J. H. et al., 1996, ApJ, 472, L9
Entel M. B., Protheroe R. J., 1995, Proc. 24th Int. Cos. Ray Conf. (Rome), Vol. 2, p. 532
Gaidos J. A. et al., 1996, Nat, 383, 319
Ghisellini G., Maraschi I., Treves A., 1985, A&A, 146, 204
Ghisellini G., Maraschi I., Dondi L., 1996, A&AS, 120, 503
Inoue S., Takahara F., 1996, ApJ, 463, 555
Jauch J. M., Rohrlich F., 1976, The theory of photons and electrons. Springer-Verlag, New York
Kerrick A. D. et al., 1995, ApJ, 438, L59
Krennrich F. et al., 1997, ApJ, 481, 758
Lin Y. C. et al., 1994, in Fichtel C. E., Gehrels N., Norris J. F., eds, Proc. AIP Symp. 304, The Second Compton Symposium. Am. Inst. Phys., New York, p. 582
Macomb D. J. et al., 1995, ApJ, 449, L99 (Erratum, 1996, ApJ, 459, L111)
Maraschi L., Ghisellini G., Celloti A., 1992, ApJ, 397, L5
Mastichiadis A., Kirk J. G., 1997, A&A, 320, 19
Meyer H., Westerhoff S., 1996, in Kirk J. G., Camenzind M., von Montigny C., Wagner S., eds, Proc. of the Heidelberg Workshop on Gamma-Ray Emitting AGN. Max-Planck Institut für Kernphysik, Heidelberg, p. 39
Mohanty G. et al., 1993, Proc. 23rd Int. cos. Ray Conf. (Calgary), Vol. 1, p. 440
Petry D. et al., 1996, A&A, 311, 13
Protheroe R. J., Stanev T., 1993, MNRAS, 264, 191
Punch M. et al., 1992, Nat, 358, 477
Quinn J. et al., 1996, ApJ, 456, L83
Schubnell M. et al., 1996, ApJ, 460, 644
Stecker F. W., De Jager O. C., Salamon M. H., 1996, ApJ, 437, L75
Stecker F. W., De Jager O. C., 1996, ApJ, 476, 712
Takahashi T. et al., 1996, ApJ, 470, L89
Zdziarski A. A., Krolik J. H., 1993, ApJ, 409, L33